Materials Letters 129 (2014) 57–60

Contents lists available at ScienceDirect

Materials Letters

journal homepage: www.elsevier.com/locate/matlet

Dipole-interaction mediated hyperthermia heating mechanism of nanostructured Fe_3O_4 composites

M.E. Sadat [a], Ronak Patel [b], Sergey L. Bud'ko [c], Rodney C. Ewing [d], Jiaming Zhang [d], Hong Xu [e], David B. Mast [a], Donglu Shi [b,f,*]

[a] Department of Physics, University of Cincinnati, Cincinnati, OH 45221, USA
[b] The Materials Science and Engineering, Dept. of Mechanical and Materials Engineering, College of Engineering and Applied Science, University of Cincinnati, Cincinnati, OH 45221, USA
[c] Ames Laboratory and Department of Physics and Astronomy, Iowa State University, Ames, IA 50011, USA
[d] Department of Geological and Environmental Sciences, University of Stanford, Stanford, CA 94305, USA
[e] Med-X Institute, Shanghai Jiao Tong University, Shanghai 200030, PR China
[f] Shanghai East Hospital, The Institute for Biomedical Engineering & Nano Science, Tongji University School of Medicine, Shanghai 200120, China.

ARTICLE INFO

Article history:
Received 14 February 2014
Accepted 2 May 2014
Available online 10 May 2014

Keywords:
Magnetism
Cancer therapy
Magnetic nanoparticle
Superparamagnetism

ABSTRACT

A correlation between the DC magnetization and hyperthermia heating rate in high frequency magnetic fields was established for two distinctively different magnetic nanoparticle (MNP) systems: (1) polystyrene (PS)/Fe_3O_4 based composites, consisting of 10 nm diameter Fe_3O_4 nanoparticles embedded in the matrix of polystyrene (PS) spheres (~100 nm), and (2) similar Fe_3O_4 nanoparticles coated with polyacrylic acid (PAA) and dispersed in water. Due to physical confinement of Fe_3O_4 nanoparticles in the former, the PS/Fe_3O_4 composite exhibited much lower magnetic hyperthermia heating compared to the latter. The reduced magnetic hyperthermia heating in the polystyrene (PS)/Fe_3O_4 based composites was found to be associated with strong dipolar interactions.

1. Introduction

In recent years, superparamagnetic nanoparticles have attracted increasing interest in biomedical research due to their unique physical and chemical properties. The ability to absorb and convert electromagnetic energy into heat has made these magnetic nanoparticles a potentially promising tool for biomedical applications especially the hyperthermia heating in cancer therapy [1–3]. Magnetic hyperthermia arises from energy loss associated with the oscillation and relaxation of the magnetic dipoles in the nanoparticles, identified as Néel and Brownian relaxations, when exposed to an alternating magnetic field [4]. Thus, if a tumor is loaded with the magnetic nanoparticles (MNP's), the local heat generated can effectively kill cancer cells; a method called magnetic hyperthermia therapeutics [5]. However, the physical mechanisms responsible for different heating behaviors among a variety of MNP systems have not been systemically identified. In particular, the key materials parameters affecting the hyperthermia heating are not well understood, including particles size, geometry, distribution, surface functionalization, and particle configuration. One such example is the observed reduction in the Specific Absorption Rate (SAR) for decreasing size of the nanoparticles in aqueous solution reported by Wang et al. [6]. They performed a series of experiments and ascribed the decrease in SAR to different particle size, surfactants, and dispersion state in the particle systems. No correlations have so far been established between the hyperthermia heating rates and MNP structural configurations for different Fe_3O_4 nanoparticles. In this work, the effects of particle–particle interaction were investigated on the hyperthermia heating performance for several Fe_3O_4 MNP's. The research was focused on magnetic relaxation behaviors associated with particle configurations, interparticle distances, confinement, and surface coatings in an applied AC magnetic field.

2. Materials and experimental details

In this work, the DC magnetization and hyperthermia heating rates of two different nanoparticle systems were investigated. The particle synthesis procedures were described in a previous report [7–9]. The first system [PS/Fe_3O_4 nanospheres (NS)] is a composite comprised of 10 nm diameter Fe_3O_4 nanoparticles that are

* Corresponding author at: College of Engineering and Applied Science, 493 Rhodes Hall, ML72, University of Cincinnati, Cincinnati, OH, 45221, USA. Tel.: +1 513 556 3100.
E-mail address: donglu.shi@uc.edu (D. Shi).

http://dx.doi.org/10.1016/j.matlet.2014.05.001
0167-577X/

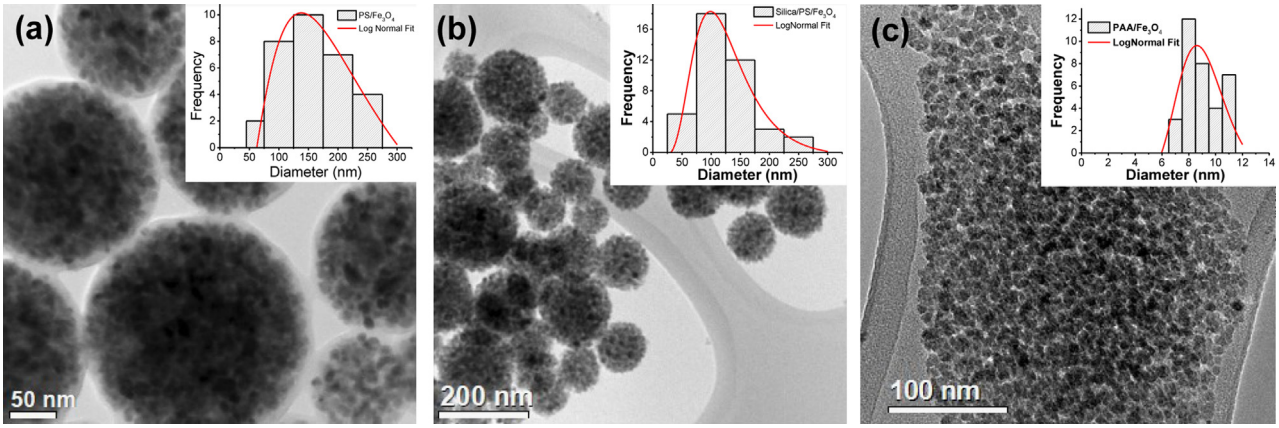

Fig. 1. TEM image of (a) Polystyrene/Fe_3O_4 nanosphere (b) Silica/Polystyrene/Fe_3O_4 nanosphere (c) PAA/Fe_3O_4 nanoparticles.

dispersed and embedded in a polystyrene (PS) matrix of a spherical shape with an average overall diameter of 100 nm [Fig. 1(a) and (b)]. Two variations of the nanospheres were studied: uncoated PS/Fe_3O_4 nanospheres [Fig. 1(a)] and the same system (Silica/PS/Fe_3O_4) [Fig. 1(b)] where the spherical polystyrene surface was coated with a thin layer of silica [7,8]. The second system of MNP's (PAA/Fe_3O_4) consists of almost same diameter Fe_3O_4 particles coated with PAA [Fig. 1(c)] [9]. Fig. 1 shows the transmission electron microscope (TEM) images of these nanoparticles and their corresponding histogram with lognormal distribution of particle size. As can be seen in this figure, the polystyrene composite materials have a spherical shape with embedded nano-size Fe_3O_4 particles. The average hydrodynamic sizes of (as measured by a Zetasizer Nano Series, Malvern instrument) the PS/Fe_3O_4, Silica/PS/Fe_3O_4 and PAA/Fe_3O_4 samples were found to be 227 nm, 191 nm and 32 nm, respectively.

The heating profiles of these MNP systems were experimentally obtained at concentrations of 0.5, 1.0, 2.5, 5 and 10 mg/mL. The heating curves were taken by placing the Fe_3O_4 MNP's in a 13.56 MHz alternating magnetic field with an amplitude of 4500 A/m, produced by a 10 turn 42 mm diameter coil. A glass vial containing the magnetic nanoparticle solution was placed inside the copper coil surrounding the Styrofoam insulation. The solution temperature was measured *in situ* as a function of time using a FISO optical fiber temperature probe (Model: FOT-L-SD). Note that a cylindrical Styrofoam surrounding the coil was used to serve as insulation for proper adiabatic conditions. After 30 min of magnetic field exposure at 4500 A/m, the temperature rise of the distilled water was no more than 1–2 °C, indicating that the samples were well isolated from the heating of the coil.

3. Results and discussion

The DC magnetization measurements of all the samples were carried out at $T=300$ K in magnitude fields up to ± 10 kOe using a SQUID magnetometer. Fig. 2(a) shows the DC magnetization curves of the PAA/Fe_3O_4 at different Fe_3O_4 concentrations and inset shows the minor hysteresis loop indicating the particles are interacting as the concentrations goes higher. The DC magnetization curves for per gram of nanoparticles for each sample are shown in Fig. 2(b) and inset shows the corresponding initial magnetization. As shown in Fig. 2(a) and (b), all magnetization curves have almost zero retentivity and coercivity indicating that the MNP systems are superparamagnetic. The magnetization (M) of an assembly of superparamagnetic particles in an external magnetic field (H) can be well described by the Langevin function

$$M = M_s L(x) = M_s\left(\coth(x) - \frac{1}{x}\right) \quad (1)$$

where M_s is the saturation magnetization, $x=\mu_o mH/k_bT$, m being the magnetic moment, μ_o is the permeability of free space, k_b is the Boltzmann constant, and T is the absolute temperature. The magnetic moment (m) can be extracted by fitting Eq. (1) with experimental magnetization curve. Assuming magnetization is unaffected by any interaction at high field, the experimental magnetization data of each sample is fitted by Eq. (1). From the fits, the obtained magnetic moments of the individual MNP's are $m=6.35\times10^{-19}$ A m^2 for PAA/Fe_3O_4, $m=2.35\times10^{-19}$ A m^2 for PS/Fe_3O_4, and $m=2.45\times10^{-19}$ A m^2 for Silica/PS/Fe_3O_4. These values are consistent to those reported by Chen et al. among which the magnetic moment of the individual 10 nm diameter PS/Fe_3O_4 was determined to be $m=2.5\times10^{-19}$ A m^2 [10]. The saturation magnetization obtained for PAA/Fe_3O_4, PS/Fe_3O_4 and Silica/PS/Fe_3O_4 samples are 61.67 emu/gm, 59.88 emu/gm and 56.85 emu/gm, respectively. Using the low field (0–100 Oe) magnetization data, the initial susceptibility (χ_i) was also found to be $\chi_i = 0.235 \pm .01(emu/(oe-gm))$ for PAA/Fe_3O_4, whereas the PS/Fe_3O_4 and Silica/PS/Fe_3O_4 samples had lower susceptibility values of $\chi_i = 0.118 \pm .014(emu/(oe-gm))$ and $\chi_i = 0.126 \pm .0022(emu/(oe-gm))$, respectively.

The time dependent temperature curve of five different concentrations of PAA/Fe_3O_4 nanoparticles exposed in AC magnetic field is shown in Fig. 3(a). The temperatures increase as a function of time and reach saturation as the heat generation is balanced by the heat loss in the MNP system. A higher saturation time was observed for higher concentrations of the Fe_3O_4 nanoparticles. As can be seen in Fig. 3(a), the initial rate of temperature change (initial slope) increases with respect to particle concentration (dashed line). The time dependent temperature curves for each sample at a fixed concentration of 10 mg/mL are shown in Fig. 3 (b). The initial heating rate per gm of Fe_3O_4 of nanoparticles for each of the concentration was also calculated and resulting plot is shown in Fig. 3(c). Interestingly, at the same magnetic volume fraction, the PAA/Fe_3O_4 material exhibited the highest heating rates by a factor of 3, compared to those of the Silica/PS/Fe_3O_4 and PS/Fe_3O_4 samples for all concentrations investigated. This behavior will have important significance in the application of hyperthermia therapy and its underlying mechanism must be identified.

The heat dissipation for an assembly of superparamagnetic particles arises due to the delay of the magnetic moment response in an AC magnetic field. Three potential mechanisms can be responsible for nanoparticles heating in AC field, namely: Néel

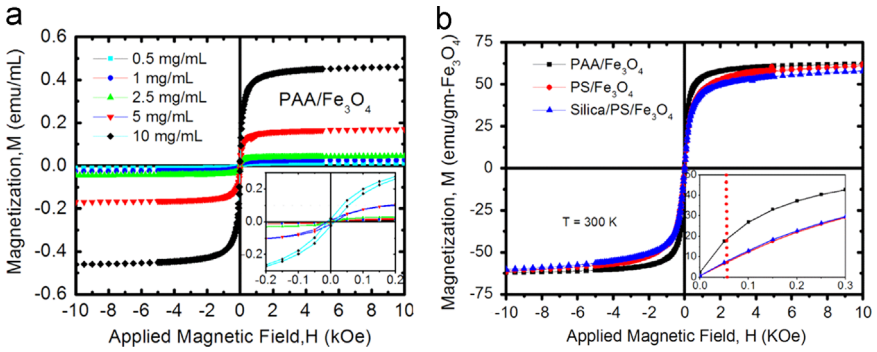

Fig. 2. (a) DC magnetization curve of PAA/Fe_3O_4 at different concentrations and inset shows the magnetization curve at low field and (b) DC magnetization curve of all NP samples and inset shows the initial magnetization where vertical dashed line indicates the field region of interest.

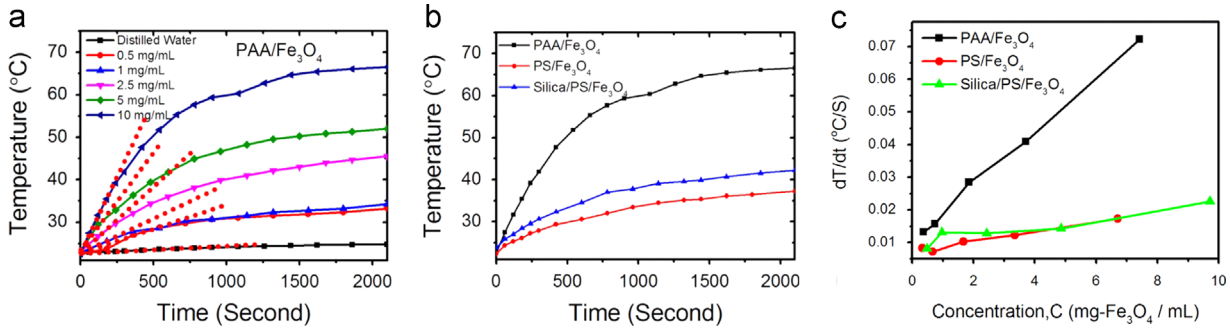

Fig. 3. (a) Heating curve of PAA/Fe_3O_4 sample for all five concentrations (b) heating curve for all three samples at a fixed concentration of 10 mg/mL (c) comparison of initial heating rate for different samples as a function of concentration.

relaxation, Brownian relaxation, and hysteresis loss [11]. PAA/Fe_3O_4 contains dispersed individual Fe_3O_4 nanoparticles that are surface coated with PAA and have the freedom to physically rotate under the AC field. However, in the PS/Fe_3O_4 and Silica/PS/Fe_3O_4 materials, the 10 nm nanoparticles are embedded in the polymer matrix of the NS and not free to individually rotate [see TEM images in Fig. 1(a) and (b)]. In this particle confinement, the Brownian relaxation is significantly reduced. However, even for quite different particle configurations, the calculated Brownian relaxation times for PAA/Fe_3O_4 and PS/Fe_3O_4 are respectively $\sim 10^{-5}$ s and $\sim 10^{-3}$ s, which is much longer than the measurement time of $\sim 10^{-8}$ s. It is therefore reasonable to eliminate the Brownian motion as the possible cause for the initial heating rate differences. Thus it is likely that most of the heat loss is arising due to the susceptibility loss (Néel relaxation process) and hysteresis loss. This hypothesis is in-fact consistent with one of the recent observation by Vallejo-Fernandez et al. They found that Néel, Brown and hysteresis losses are all effective in NP's heating in AC magnetic field for a polydisperse sample [11]. However, in the case of NS samples, as the particles are closely packed and confined in PS matrix, in addition to the suppressed Brownian loss, they might experience strong dipole interactions. Therefore, it is very difficult to thermally activate the nanoparticles at such small field. So most of the heat losses in NS systems are likely due to the hysteresis loss. However, PAA/Fe_3O_4 nanoparticles are more relaxed and particles can move freely. Therefore their magnetic moment can switch in presence of AC field. In this situation, both Néel relaxation and hysteresis loss contribute to the overall heating performance.

The minor hysteresis loop area calculated for PAA/Fe_3O_4, PS/Fe_3O_4 and Silica/PS/Fe_3O_4 samples at 10 mg/mL concentrations are 10.63 (a.u), 4.95 (a.u), 7.65 (a.u), respectively. These would be sufficient dissipations that are responsible for hyperthremia heating. The experimental results shown in Figs. 2 and 3 indicate a close correlation between the initial magnetization and heating rate. Both are dependent on concentration, which can be explained by the theory of Rosensweig [12]. According to Rosensweig, the loss power is scaled to the initial susceptibility. More detailed study on the magnetic hyperthermia mechanism of different Fe_3O_4 systems is currently under way.

4. Conclusions

In conclusion, the mechanisms governing the magnetic heating behavior of different Fe_3O_4 nanoparticle systems have been identified. It is found that, for the same volume fraction of magnetic materials, the initial heating rate is much lower in the polystyrene (PS)/Fe_3O_4 based composites where the Fe_3O_4 nanoparticles are physically confined in the polystyrene matrix. In contrast, in the PAA/Fe_3O_4, the high heating rate is due to weak dipolar interactions and higher hysteresis loss. It is concluded that, for more efficient magnetic hyperthermia heating, the dipole interaction is the key factor that should be reduced in the design and synthesis of Fe_3O_4 nanomaterials.

Acknowledgments

Work at the Ames Laboratory was supported by the Department of Energy, Basic Energy Sciences, Division of Materials Sciences and Engineering under contract no. DE-AC02-07CH11358. The work at University of Cincinnati was supported by a National Science Foundation (NSF) grant under contract no. NSF (1343568). The work

at Tongji University was supported by grants from Shanghai Nanotechnology Promotion Center (12nm0501201, 11nm0506100) and the National Natural Science Foundation of China (51173135).

References

[1] Pankhurst QA, Connolly J, Jones SK, Dobson J. J Phys D: Appl Phys 2003;36:R167.
[2] Hergt R, Dutz S, Müller R, Zeisberger M. J Phys Condens Matter 2006;18:S2919.
[3] Laurent S, Dutz S, Häfeli UO, Mahmoudi M. Adv Colloid Interface Sci 2011;166:8–23.
[4] Jordan A, Scholz R, Wust P, Fähling H, Felix R. J Magn Magn Mater 1999;201:413–9.
[5] Kumar CS, Mohammad F. Adv Drug Delivery Rev 2011;63:789–808.
[6] Wang X, Gu H, Yang Z. J Magn Magn Mater 2005;293:334–40.
[7] Molday RS. Patent 4,452,773, 1984. U.S. Patent 1984;4,452,773.
[8] Xu H, Cui L, Tong N, Gu H. J Am Chem Soc 2006;128:15582–3.
[9] Xu F, Cheng C, Chen D, Gu H. Chem Phys Chem 2012;13:336–41.
[10] Chen D, Sanchez A, Xu H, Gu H, Shi D. J Appl Phys 2008;104:093902.
[11] Vallejo-Fernandez G, Whear O, Roca A, Hussain S, Timmis J, Patel V, et al. J Phys D: Appl Phys 2013;46:312001.
[12] Rosensweig RE. J Magn Magn Mater 2002;252:370–4.